



Bio-catalysts and catalysts based on ruthenium(II) polypyridyl complexes imparting diphenyl-(2-pyridyl)-phosphine as a co-ligand

Prashant Kumar, Ashish Kumar Singh, Rampal Pandey, Daya Shankar Pandey*

Department of Chemistry, Faculty of Science, Banaras Hindu University, Varanasi, U.P. 221 005, India

ARTICLE INFO

Article history:

Received 14 February 2011

Received in revised form

7 June 2011

Accepted 28 June 2011

Keywords:

Polypyridyl ruthenium complex

Topo II isomerase inhibition

DNA binding

Catalysis

Diphenylphosphinopyridine

ABSTRACT

Reactions of the ruthenium complexes $[\text{Ru}(\kappa^3\text{-tpy})(\text{PPh}_3)_2\text{Cl}_2]$, $[\text{Ru}(\kappa^3\text{-tptz})(\text{PPh}_3)_2\text{Cl}_2]$ and $[\text{Ru}(\kappa^3\text{-tpy})\text{Cl}_3]$ [$\text{tpy} = 2,2':6',2''\text{-terpyridine}$; $\text{tptz} = 2,4,6\text{-tris}(2\text{-pyridyl})\text{-1,3,5-triazine}$] with diphenyl-(2-pyridyl)-phosphine (PPh_2Py) have been investigated. The complexes $[\text{Ru}(\kappa^3\text{-tpy})(\text{PPh}_3)_2\text{Cl}_2]$ and $[\text{Ru}(\kappa^3\text{-tptz})(\text{PPh}_3)_2\text{Cl}_2]$ reacted with PPh_2Py to afford $[\text{Ru}(\kappa^3\text{-tpy})(\kappa^1\text{-P-PPh}_2\text{Py})_2\text{Cl}]^+$ (**1**) and $[\text{Ru}(\kappa^3\text{-tptz})(\kappa^1\text{-P-PPh}_2\text{Py})_2\text{Cl}]^+$ (**2**), which were isolated as their tetrafluoroborate salts. Under analogous conditions, $[\text{Ru}(\kappa^3\text{-tpy})\text{Cl}_3]$ gave a neutral complex $[\text{Ru}(\kappa^3\text{-tpy})(\kappa^1\text{-PPh}_2\text{Py})\text{Cl}_2]$ (**3**). Upon treatment with an excess of NH_4PF_6 in methanol, **1** and **2** gave $[\text{Ru}(\kappa^3\text{-tpy})(\kappa^1\text{-P-PPh}_2\text{Py})(\kappa^2\text{-P,N-PPh}_2\text{Py})](\text{PF}_6)_2$ (**4**) and $[\text{Ru}(\kappa^3\text{-tptz})(\kappa^1\text{-P-PPh}_2\text{Py})(\kappa^2\text{-P,N-PPh}_2\text{Py})](\text{PF}_6)_2$ (**5**) containing both monodentate and chelated PPh_2Py . Further, **4** and **5** reacted with an excess of NaCN and CH_3CN to afford $[\text{Ru}(\kappa^3\text{-tpy})(\kappa^1\text{-P-PPh}_2\text{Py})_2(\text{CN})](\text{PF}_6)$ (**6**), $[\text{Ru}(\kappa^3\text{-tpy})(\kappa^1\text{-P-PPh}_2\text{Py})_2(\text{NCCH}_3)](\text{PF}_6)_2$ (**7**), $[\text{Ru}(\kappa^3\text{-tptz})(\kappa^1\text{-P-PPh}_2\text{Py})_2(\text{CN})]\text{PF}_6$ (**8**) and $[\text{Ru}(\kappa^3\text{-tptz})(\kappa^1\text{-P-PPh}_2\text{Py})_2(\text{NCCH}_3)](\text{PF}_6)_2$ (**9**) supporting hemilabile nature of the coordinated PPh_2Py . The complexes have been characterized by elemental analyses, spectral (IR, NMR, electronic absorption, FAB-MS), electrochemical studies and structures of **1**, **2** and **3** determined by X-ray single crystal analyses. At higher concentration level (40 μM) the complexes under investigation exhibit inhibitory activity against DNA-Topo II of the filarial parasite *S. cervi* and **3** catalyses rearrangement of aldoximes to amide under aerobic conditions.

© 2011 Elsevier B.V. All rights reserved.

1. Introduction

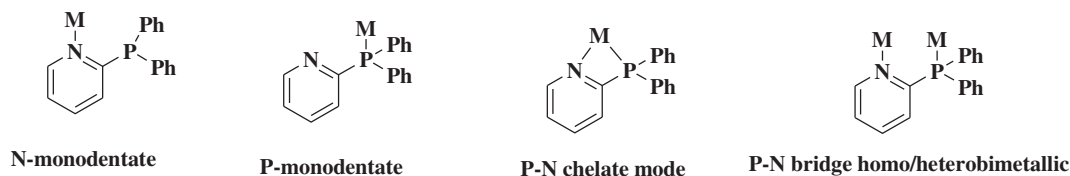
Considerable current interest has arisen in ruthenium(II) polypyridyl complexes because of their interesting photochemical properties and potential application in diverse areas [1–6]. The cationic complexes based on Pt, Ru, Rh, Co and Zn containing polypyridyl ligands display intense metal-to-ligand charge transfer (MLCT) and strong luminescence in the visible region and have the potential to serve as an excellent probe for various micro-environments [7,8]. The polypyridyl ligands present in complexes play an important role in determining and improving their light emitting and electron transfer performances [9–11]. Study of kinetically inert octahedral Ru(II) complexes as chiral probes for DNA has elicited intense investigation in recent years. The Ru(II) complexes may bind DNA either through non-covalent interactions such as electrostatic, groove binding and intercalation, or a combination of these depending upon its structure [12,13]. An understanding of how the metal complexes bind DNA will not only pave the way to understand fundamentals of these interactions but, also,

about a variety of potential applications. DNA-topoisomerases, which are intricately involved in maintaining the topographic structure of DNA transcription and mitosis, have been identified as an important biochemical target in cancer chemotherapy, microbial infection, and development of antifilarial compounds [14–16]. In our earlier work we have shown that octahedral ruthenium complexes containing both the phosphine and polypyridyl/pyridylazine ligands behave as Topo II inhibitors and inhibition percentage largely depends on the nature of complexes and number of uncoordinated N-donor sites of the polypyridyl ligand [14–17].

The hetero difunctional ligand diphenyl-(2-pyridyl)-phosphine (PPh_2Py) may coordinate metal center in monodentate, chelating or bridging manner depending on requirements (Scheme 1) [18–23]. PPh_2Py , in its chelating mode forms four membered rings which are strained, relatively unstable, and plays crucial role in catalysis [24–33]. While a few reports dealing with ruthenium complexes based on PPh_2Py are available in the literature complexes containing both the PPh_2Py and polypyridyl ligands are rather scarce [18–23].

Transition metal-catalyzed transfer hydrogenations have been successfully employed in the transformation of alcohol and

* Corresponding author. Tel.: +91 542 6702480; fax: +91 542 2368174.
E-mail addresses: dspbhu@bhu.ac.in, dspbhu@yahoo.co.in (D. S. Pandey).



Scheme 1.

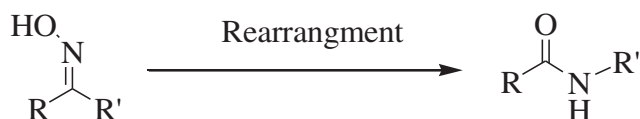
carbonyl compounds [34–38]. Catalytic reduction of alkenes and imines has also been achieved in presence of an alcohol as stoichiometric reducing agent, as the conversion of alcohol into amine using ruthenium catalysts [34–39]. The rearrangement of oxime to amide is catalyzed by many reagents and generally in such reactions R group *anti*- to the hydroxyl migrates to give the final product (Scheme 2). Metal-catalyzed rearrangement of aldoximes is well documented in the literature and it has been shown that these reactions require relatively high catalyst loadings and elevated temperature [34–38]. Recently, Williams et al., have reported a catalyst based on ruthenium that effectively catalyses rearrangement of aldoximes to amides [39]. This catalytic system requires both a chelating phosphine and *p*-toluene sulfonic acid as an additive and can form a mixture of amide and nitrile.

It is noteworthy that the ligand tpy is indispensable in coordination chemistry and molecular recognition, complexes based on it has seldom been employed in organometallic catalysis [40–47]. In this direction, an attempt has been made to develop bio-catalysts and catalysts based on ruthenium complexes containing both PPh₂Py and polypyridyl ligands tpy or tptz. The present work deals with synthesis and characterization of cationic ruthenium(II) complexes of the formulations [Ru(κ^3 -L)(κ^1 -P-PPh₂Py)₂Cl]⁺ (L = tpy or tptz), [Ru(κ^3 -L)(κ^1 -P-PPh₂Py)(κ^2 -P,N-PPh₂Py)]²⁺, a neutral complex [Ru(κ^3 -tpy)(κ^1 -PPh₂Py)Cl₂] and crystal structures of [Ru(κ^3 -tpy)(κ^1 -P-PPh₂Py)₂Cl]BF₄ (**1**), [Ru(κ^3 -tptz)(κ^1 -P-PPh₂Py)₂Cl]BF₄ (**2**), and [Ru(κ^3 -tpy)(κ^1 -PPh₂Py)-Cl₂] (**3**). We also report herein, inhibitory effect of **1–5** on DNA-Topoisomerase (Topo II) activity of the filarial parasite *Setaria. cervi*, β -hematin/hemozoin formation in presence of *Plasmodium yoelii* lysate and application of **3** in the rearrangement of aldoximes to amide under aerobic conditions.

2. Experimental section

2.1. General

Analytical grade reagents were used throughout. The solvents were dried and distilled following standard literature procedures [48]. Hydrated ruthenium(III) chloride, diphenyl-(2-pyridyl)-phosphine, 2,2':6',2''-terpyridine, 2,4,6-tris(2-pyridyl)-1,3,5-triazine, ammonium tetrafluoroborate and ammonium hexafluorophosphate were procured from Aldrich and used without further purifications. Calf thymus (CT) and supercoiled pBR322 DNA were procured from Sigma Chemical Co., St. Louis, MO. The complexes [Ru(κ^3 -tpy)Cl₂(PPh₃)], [Ru(κ^3 -tptz)Cl₂(PPh₃)] and [Ru(κ^3 -tpy)Cl₃] were prepared following literature procedures [17,49]. Various buffers were prepared in triply distilled deionized



Scheme 2. Beckmann rearrangement of oximes to amides.

water. Topoisomerase II (Topo II) was isolated from the filarial parasite *S. cervi* and partially purified by literature procedures [50,51].

2.2. Instrumentation

Elemental analyses for C, H and N were performed on an Exeter CE-440 elemental analyzer. Infra red spectra in nujol mull and electronic spectra in dichloromethane were acquired on a Varian 3300 FT-IR and Shimadzu UV-1601 spectrophotometers, respectively. ¹H and ³¹P NMR spectra were obtained at room temperature on a JEOL AL 300 FT-NMR using CDCl₃ as a solvent and TMS as an internal reference for ¹H and 85% H₃PO₄ for ³¹P NMR. FAB mass spectra (FAB-MS) were recorded on a JOEL SX 102/DA-6000 Mass Spectrometer using Xenon as the FAB gas (6 kV, 10 mA). Accelerating voltage was 10 kV and spectra were recorded at room temperature using *m*-nitrobenzyl alcohol as the matrix. Cyclic voltammetric measurements were performed on a CHI 620c electrochemical analyzer. A platinum working electrode, platinum wire auxiliary electrode, and Ag/Ag⁺ reference electrode were used in a standard three electrode configuration. Tetrabutylammonium perchlorate (TBAP) was used as the supporting electrolyte and solution concentration was ca. 10⁻³.

2.3. Synthesis

2.3.1. Synthesis of [Ru(κ^3 -tpy)(κ^1 -P-PPh₂Py)₂Cl]BF₄ (**1**)

To a suspension of [Ru(κ^3 -tpy)(PPh₃)Cl₂] (0.667 g, 1.0 mmol) in methanol (25 mL) PPh₂Py (0.526 g, 2.0 mmol) was added and contents of the flask were heated under reflux for 07 h. Resulting dark red solution was cooled to room temperature and filtered to remove any solid residue. The filtrate was concentrated to one fourth of its volume under reduced pressure and a saturated solution of ammonium tetrafluoroborate dissolved in methanol added to it. Slowly, microcrystalline product separated which was filtered washed with diethyl ether and dried under *vacuo*. Yield: 0.339 g (77%). Microanalytical data BC₄₉F₄H₃₉N₅P₂RuCl requires: C, 55.01; H, 3.67; N, 6.55%. Found: C, 55.15; H, 3.59; N, 6.44%. FAB-MS [*m/z*, calcd. (obs.)]: 983.1 (983) [Ru(tpy)(PPh₂Py)₂Cl](BF₄); 896.3 (896) [Ru(tpy)(PPh₂Py)₂Cl]⁺; 860.8 (860) [Ru(tpy)(PPh₂Py)₂]²⁺; 597.8 (597) [Ru(tpy)(PPh₂Py)]²⁺. ¹H NMR (δ ppm): 8.91 (d, 2H, *J* = 5.1 Hz, tpy), 8.69 (d, 2H, *J* = 5.4 Hz; Py, PPh₂Py), 8.47 (d, 2H, *J* = 6.3 Hz, tpy), 8.13 (d, 2H, *J* = 6.9 Hz; Py, PPh₂Py), 7.94 (d, 3H, *J* = 7.8 Hz; Py, PPh₂Py + tpy), 7.71 (d, 4H, *J* = 6.0 Hz, tpy), 7.45 (d, 2H, *J* = 4.8 Hz, tpy), 7.26–6.92 (br. m, 20H, PPh₂Py), 6.45 (d, 2H, *J* = 6.3 Hz; Py, PPh₂Py). ³¹P{¹H} NMR (δ ppm): 36.02 (s). IR (nujol, cm⁻¹): 1626 (s), 1440 (s), 1394 (m), 1102 (m), 758 (s), 698 (s), 1056 (br, B–F, BF₄). UV–vis [λ_{\max} , nm; ϵ , M⁻¹ cm⁻¹]: 554 (10800), 485 (21000), 345 (19400), 286 (39500).

2.3.2. Synthesis of [Ru(κ^3 -tptz)(κ^1 -P-PPh₂Py)₂Cl]BF₄ (**2**)

It was prepared following the above procedure for **1** using [Ru(κ^3 -tptz)Cl₂(PPh₃)] in place of [Ru(κ^3 -tpy)(PPh₃)Cl₂]. Yield: 0.524 g (70%). Microanalytical data BC₅₂F₄H₄₀N₈P₂O₂ClRu requires: C, 57.08; H, 3.68; N, 10.24%. Found: C, 56.98; H, 3.71; N, 10.22%. FAB-

MS [m/z , calcd. (obs.)]: 1007.4 (1008) $[\text{Ru}(\text{tptz})(\text{PPh}_2\text{Py})_2\text{Cl}]^+$; 744.14 (745) $[\text{Ru}(\text{tptz})(\text{PPh}_2\text{Py})\text{Cl}]^+$; 480.8 (481) $[\text{Ru}(\text{tptz})\text{Cl}]^+$. ^1H NMR (δ ppm): 9.20 (d, 2H, $J = 3.9$ Hz, tptz), 8.84 (d, 1H, $J = 7.8$ Hz, tptz), 8.78 (d, 2H, $J = 6.3$ Hz; Py, PPh₂Py), 8.74 (d, 2H, $J = 11.7$ Hz; Py, PPh₂Py), 8.60 (d, 3H, $J = 6.0$ Hz, tptz), 8.43 (d, 2H, $J = 5.1$ Hz, tptz), 8.17 (d, 2H, $J = 5.1$ Hz, tptz), 7.85 (d, 2H, $J = 6.3$ Hz; Py, PPh₂Py), 7.65 (d, 2H, $J = 4.8$ Hz, tptz), 7.08–7.40 (br. m, 20H, PPh₂Py), 6.37 (d, 2H, $J = 7.5$ Hz; Py, PPh₂Py). $^{31}\text{P}\{^1\text{H}\}$ NMR (δ ppm): 40.40 (s). IR (nujol, cm^{-1}): 1596 (s), 1436 (s), 1390 (m), 1108 (m), 748 (s), 692 (s), 1054 (br, BF_4^-). UV–vis. [λ_{max} , nm; ϵ , $\text{M}^{-1}\text{cm}^{-1}$]: 536 (7940), 481 (11900), 346 (24100), 241 (38400).

2.3.3. Synthesis of $[\text{Ru}(\kappa^3\text{-tpy})(\kappa^1\text{-P-PPh}_2\text{Py})\text{Cl}_2]$ (**3**)

PPh₂Py (0.263 g, 1.0 mmol) was added to a suspension of $[\text{Ru}(\kappa^3\text{-tpy})\text{Cl}_3]$ (0.439 g, 1.00 mmol) in methanol (25 mL) and heated under reflux for 07 h. Resulting solution was cooled to room temperature and filtered to remove any solid residue. The filtrate was concentrated under reduced pressure to one fourth of its volume and left undisturbed for slow crystallization. Slowly, a microcrystalline product separated which was filtered washed with diethyl ether and dried under *vacuo*. Its crystal contained one CH_2Cl_2 molecule. Yield: 0.169 g (64%). Microanalytical data $\text{C}_{33}\text{H}_{27}\text{N}_4\text{P}_2\text{Cl}_4\text{Ru}$ requires: C, 52.61; H, 3.61; N, 7.44%. Found: C, 52.54; H, 3.56; N, 7.42%. FAB-MS [m/z , obs. (calcd.)]: 668 $[\text{Ru}(\text{tpy})(\text{PPh}_2\text{Py})\text{Cl}_2]^+$; 405 $[\text{Ru}(\text{tpy})\text{Cl}_2]^+$. ^1H NMR (δ ppm): 9.18 (d, 2H, $J = 3.9$ Hz, tpy), 8.93 (d, 1H, $J = 4.2$ Hz; Py, PPh₂Py), 8.71 (d, 2H, $J = 6.9$ Hz, tpy), 8.45 (d, 1H, $J = 5.7$ Hz; Py, PPh₂Py), 8.01 (t, 3H, $J = 6.7$ Hz; Py, PPh₂Py + tpy), 7.82 (dd, 3H, $J = 3.9$ Hz, tpy), 7.62 (t, 2H, $J = 6.1$ Hz, tpy), 6.99–7.45 (br. m, 10H, PPh₂Py), 6.34 (t, 1H, $J = 6.3$ Hz; Py, PPh₂Py). $^{31}\text{P}\{^1\text{H}\}$ NMR (δ ppm): 42.87 (s). IR (nujol, cm^{-1}): 1624 (s), 1436 (s), 1396 (m), 1116 (m), 752 (s), 688 (s). UV–vis. [λ_{max} , nm; ϵ , $\text{M}^{-1}\text{cm}^{-1}$]: 548 (5520), 496 (9870), 354 (96300), 275 (27100).

2.3.4. Synthesis of $[\text{Ru}(\kappa^3\text{-tpy})(\kappa^1\text{-P-PPh}_2\text{Py})(\kappa^2\text{-P,N-PPh}_2\text{Py})](\text{PF}_6)_2$ (**4**)

NH_4PF_6 (0.354 g, 2.0 mmol) was added to suspension of **1** (1.069 g, 1.0 mmol) in methanol (15 mL) and stirred at room temperature for 08 h. It gave a clear red solution which was concentrated to dryness on a rotatory evaporator, extracted with dichloromethane and filtered. The filtrate was saturated with petroleum ether and left undisturbed for slow crystallization. Slowly, microcrystalline solid separated which was filtered, washed with diethyl ether and dried in *vacuo*. Yield 0.664 g (57%). Microanalytical data $\text{C}_{49}\text{F}_{12}\text{H}_{39}\text{N}_5\text{P}_4\text{Ru}$ requires: C, 51.14; H, 3.42; N, 6.09%. Found: C, 51.11; H, 3.44; N, 6.12%. FAB-MS [m/z , calcd. (obs.)]: 860.9 (860) $[\text{Ru}(\text{tpy})(\text{PPh}_2\text{Py})(\text{PPh}_2\text{Py})]^+$; 597.6 (597) $[\text{Ru}(\text{tpy})(\text{PPh}_2\text{Py})]^+$. ^1H NMR (δ ppm): 8.74 (d, 2H, $J = 4.8$ Hz, tpy), 8.26 (d, 1H, $J = 6.0$ Hz; Py, $\kappa^2\text{-PPh}_2\text{Py}$), 8.10 (d, 3H, $J = 7.8$ Hz; Py, $\kappa^1\text{-PPh}_2\text{Py} + \text{tpy}$), 7.91 (t, 3H, $J = 7.6$ Hz; Py, PPh₂Py + tpy), 7.84 (d, 2H, $J = 7.8$ Hz, tpy), 7.61 (d, 4H, $J = 3.9$ Hz; Py, PPh₂Py + tpy), 7.49 (d, 2H, $J = 4.2$ Hz, tpy), 7.08–7.33 (br. m, 20H, PPh₂Py), 6.80 (q, 1H, $J = 6.3$ Hz; Py, PPh₂Py), 6.45 (t, 1H, $J = 6.3$ Hz; Py, PPh₂Py). $^{31}\text{P}\{^1\text{H}\}$ NMR (δ ppm): 36.42 (s), –10.30 (s). IR (nujol, cm^{-1}): 1620 (s), 1439 (s), 1393 (m), 1100 (m), 768 (s), 694 (s), 840 (s, PF_6^-). UV–vis. [λ_{max} , nm; ϵ , $\text{M}^{-1}\text{cm}^{-1}$]: 539 (9270), 484 (17800), 341 (15700), 243 (38700).

2.3.5. Synthesis of $[\text{Ru}(\kappa^3\text{-tptz})(\kappa^1\text{-P-PPh}_2\text{Py})(\kappa^2\text{-P,N-PPh}_2\text{Py})](\text{PF}_6)_2$ (**5**)

It was prepared following the above procedure for **2** using $[\text{Ru}(\kappa^3\text{-tptz})(\kappa^1\text{-P-PPh}_2\text{Py})_2\text{Cl}]\text{BF}_4$ (1.094 g, 1.00 mmol) in place of $[\text{Ru}(\kappa^3\text{-tpy})(\kappa^1\text{-P-PPh}_2\text{Py})_2\text{Cl}]\text{BF}_4$. Yield: 0.750 g (68%). Microanalytical data $\text{C}_{52}\text{H}_{40}\text{N}_8\text{P}_4\text{F}_{12}\text{Ru}$ requires: C, 50.78; H, 3.28; N, 9.11%. Found: C, 50.74; H, 3.26; N, 9.14%. FAB-MS [m/z , obs. (calcd.)]: 1084

$[\text{Ru}(\text{tptz})(\text{PPh}_2\text{Py})(\text{PPh}_2\text{Py})]^+$; 821 $[\text{Ru}(\text{tptz})(\text{PPh}_2\text{Py})]^+$. ^1H NMR (δ ppm): 9.02 (d, 2H, $J = 6.1$ Hz, tptz), 8.79 (d, 1H, $J = 6.3$ Hz; Py, $\kappa^2\text{-PPh}_2\text{Py}$), 8.65 (d, 1H, $J = 4.2$ Hz; Py, $\kappa^1\text{-PPh}_2\text{Py}$), 8.43 (d, 2H, $J = 5.4$ Hz, tptz), 7.97 (d, 6H, $J = 4.8$ Hz; Py, PPh₂Py + tptz), 7.90 (d, 2H, $J = 6.9$ Hz; Py, PPh₂Py), 7.85 (d, 4H, $J = 6.3$ Hz, tptz), 6.97–7.36 (br. m, 20H, PPh₂Py), 6.35 (d, 2H, $J = 7.5$ Hz; Py, PPh₂Py). $^{31}\text{P}\{^1\text{H}\}$ NMR (δ ppm): –12.30 (s), 38.48 (s). IR (nujol, cm^{-1}): 1598 (s), 1439 (s), 1388 (m), 1112 (m), 758 (s), 698 (s), 845 (s, PF_6^-). UV–vis. [λ_{max} , nm; ϵ , $\text{M}^{-1}\text{cm}^{-1}$]: 538 (6479), 495 (11900), 358 (10300), 279 (34400), 239 (35300).

2.3.6. Synthesis of $[\text{Ru}(\kappa^3\text{-tpy})(\kappa^1\text{-P-PPh}_2\text{Py})_2(\text{CN})](\text{PF}_6)_2$ (**6**)

NaCN (0.52 g, 8.0 mmol) was added to a suspension of **2** (0.1 g, 0.086 mmol) in methanol (40 mL) and contents of the flask heated under reflux for 10 h. Resulting solution was concentrated to dryness under reduced pressure and the residue extracted with dichloromethane (40 mL). After filtration through celite, the filtrate was saturated with diethyl ether. It gave a red solid which was filtered, washed with diethyl ether and dried in air. Yield: 0.670 g (64%). Microanalytical data $\text{C}_{50}\text{H}_{39}\text{N}_6\text{P}_3\text{F}_6\text{Ru}$ requires: C, 58.20; H, 3.81; N, 8.14%. Found: C, 58.42; H, 4.13; N, 8.04%. ^1H NMR (δ ppm): 8.45 (d, 2H, $J = 4.2$ Hz, tpy), 7.86 (d, 2H, $J = 7.2$ Hz; Py, PPh₂Py), 7.74 (m, 5H; Py, PPh₂Py + tpy), 7.64 (t, 4H, $J = 8.1$ Hz, tpy), 7.48 (t, 4H, $J = 8.1$ Hz; Py, PPh₂Py + tpy), 7.36–6.94 (br. m, 20H, PPh₂Py), 6.87 (t, 2H, $J = 6.3$ Hz; Py, PPh₂Py). $^{31}\text{P}\{^1\text{H}\}$ NMR (δ ppm): 36.72 (s). IR (nujol, cm^{-1}): 2224 (s, $\nu(\text{C}\equiv\text{N})$), 1625 (s), 1441 (s), 1393 (m), 1102 (m), 756 (s), 698 (s), 844 (s, PF_6^-).

2.3.7. Synthesis of $[\text{Ru}(\kappa^3\text{-tpy})(\kappa^1\text{-P-PPh}_2\text{Py})_2(\text{NCCH}_3)](\text{PF}_6)_2$ (**7**)

It was prepared following the above procedure for **6** except that an excess of CH_3CN was used in place of NaCN. Yield: 0.882 g, 74%. Microanalytical data: $\text{C}_{51}\text{H}_{42}\text{N}_6\text{P}_4\text{F}_{12}\text{Ru}$ requires: C, 51.39; H, 3.55; N, 7.05%. Found: C, 51.36; H, 3.44; N, 7.03%. ^1H NMR (δ ppm): 8.44 (d, 2H, $J = 4.3$ Hz, tpy), 7.84 (d, 4H, $J = 7.5$ Hz; Py, PPh₂Py), 7.72 (m, 7H; Py, PPh₂Py + tpy), 7.60 (t, 2H, $J = 7.5$ Hz, tpy), 7.48 (t, 2H, $J = 7.8$ Hz, tpy), 7.26–7.04 (br. m, 20H, PPh₂Py), 6.87 (t, 2H, $J = 6.3$ Hz; Py, PPh₂Py), 2.18 (s, 3H, CH_3). $^{31}\text{P}\{^1\text{H}\}$ NMR (δ ppm): 36.72 (s). IR (nujol, cm^{-1}): 2100 (s, $\nu(\text{C}\equiv\text{N})$), 1628 (s, $\nu(\text{C}=\text{N})$), 1439 (s), 1396 (m), 1100 (m), 756 (s), 698 (s), 842 (s, PF_6^-).

2.3.8. Synthesis of $[\text{Ru}(\kappa^3\text{-tptz})(\kappa^1\text{-P-PPh}_2\text{Py})_2(\text{CN})](\text{PF}_6)_2$ (**8**)

NaCN (0.39 g, 8.0 mmol) was added to a suspension of **4** (0.1 g, 0.081 mmol) in methanol (40 mL) and refluxed for 10 h. Resulting solution was concentrated to dryness under reduced pressure and residue extracted with dichloromethane (40 mL). After filtration through celite the filtrate was saturated with diethyl ether. It gave a brown red solid which was filtered, washed with diethyl ether and dried in air. Yield: 0.810 g, 72%. Microanalytical data: $\text{C}_{54}\text{H}_{44}\text{N}_9\text{P}_3\text{F}_6\text{Ru}$ requires: C, 57.55; H, 3.94; N, 11.19%. Found: C, 57.46; H, 3.76; N, 11.11%. ^1H NMR (δ ppm): 8.96 (d, 2H, $J = 2.6$ Hz, tptz), 8.78 (d, 1H, $J = 6.4$ Hz, tptz), 8.72 (d, 2H, $J = 6.0$ Hz; Py, PPh₂Py), 8.68 (d, 2H, $J = 9.8$ Hz; Py, PPh₂Py), 8.54 (d, 3H, $J = 6.2$ Hz, tptz), 8.48 (d, 2H, $J = 5.0$ Hz, tptz), 8.20 (d, 2H, $J = 4.8$ Hz, tptz), 7.80 (d, 2H, $J = 5.8$ Hz; Py, PPh₂Py), 7.52 (d, 2H, $J = 3.8$ Hz, tptz), 7.12–7.36 (br. m, 20H, PPh₂Py), 6.48 (d, 2H, $J = 5.6$ Hz; Py, PPh₂Py). $^{31}\text{P}\{^1\text{H}\}$ NMR (δ ppm): 42.54 (s). IR (nujol, cm^{-1}): 2221 (s, $\nu(\text{C}\equiv\text{N})$), 1594 (s, $\nu(\text{C}=\text{N})$), 1439 (s), 1390 (m), 1115 (m), 758 (s), 712 (s), 846 (s, P–F, PF_6^-). UV–vis. [λ_{max} , nm; ϵ , $\text{M}^{-1}\text{cm}^{-1}$]: 516 (9600), 355 (15200), 274 (30100).

2.3.9. Synthesis of $[\text{Ru}(\kappa^3\text{-tptz})(\kappa^1\text{-P-PPh}_2\text{Py})_2(\text{CH}_3\text{CN})](\text{PF}_6)_2$ (**9**)

It was prepared following the above procedure for **8** except that an excess CH_3CN was used in place of NaCN. Yield: 0.876 g, 69%. Microanalytical data: $\text{C}_{54}\text{H}_{43}\text{N}_9\text{P}_4\text{F}_{12}\text{Ru}$ requires: C, 51.03; H, 3.41; N, 9.92%. Found: C, 50.97; H, 3.32; N, 9.76%. ^1H NMR (δ ppm): 9.08

(d, 2H, $J = 3.6$ Hz, tptz), 8.92 (d, 1H, $J = 6.4$ Hz, tptz), 8.70 (d, 2H, $J = 5.8$ Hz; Py, PPh₂Py), 8.66 (d, 2H, $J = 8.6$ Hz; Py, PPh₂Py), 8.60 (d, 3H, $J = 5.2$ Hz, tptz), 8.38 (d, 2H, $J = 4.8$ Hz, tptz), 8.08 (d, 2H, $J = 4.2$ Hz, tptz), 7.76 (d, 2H, $J = 5.8$ Hz; Py, PPh₂Py), 7.55 (d, 2H, $J = 3.6$ Hz, tptz), 7.04–7.30 (br. m, 20H, PPh₂Py), 6.38 (d, 2H, $J = 6.6$ Hz; Py, PPh₂Py), 2.21 (s, 3H, CH₃). ³¹P{¹H} NMR (δ ppm): 39.82 (s). IR (nujol, cm⁻¹): 2112 {s, ν (C \equiv N)}, 1600 (s), 1436 (s), 1392 (m), 1108 (m), 752(s), 694 (s), 840 (s, PF₆⁻). UV–vis. [λ_{\max} , nm; ϵ , M⁻¹ cm⁻¹]: 544 (9450), 374 (18770), 282 (23700).

2.4. Catalytic activity

Mixture of the oxime (2.0 mmol) and the catalyst [Ru(κ^3 -tpy)(κ^1 -P-PPh₂Py)Cl₂] (**3**) (13.3 mg, 0.02 mmol) was refluxed in toluene (1 mL) for appropriate time (Table 1). After completion of the reaction CH₂Cl₂ was added to reaction mixture and resulting solution was filtered through celite. The crude product was purified by column chromatography (silica gel, MeOH/CH₂Cl₂). After work-up amides were obtained in good yield (Table 1).

2.5. X-ray structural analysis

Crystals suitable for single crystal X-ray diffraction analyses for **1**, **2** and **3** were obtained by slow diffusion of petroleum ether (40–60 °C) to the solution of respective complexes in CH₂Cl₂ at room temperature. Preliminary data on the space group and unit cell dimensions as well as intensity data were collected on Oxford Diffraction X CALIBUR-S and Bruker Smart APEX II diffractometer using graphite monochromatized Mo-K α radiation. Structures were solved by direct methods and refined using SHELX-97 [52]. The non-hydrogen atoms were refined with anisotropic thermal parameters. Hydrogen atoms were geometrically fixed and allowed to refine using riding model. Computer program PLATON was used for analyzing interaction and stacking distances [53].

2.6. Absorption titration

Absorption titration studies were performed using a constant concentration of CT-DNA (20 μ M) in aqueous tris buffer (5 mM Tris–HCl, 50 mM NaCl; 7.1 pH) and varying the concentration of complexes in spectral region 340–250 nm.

2.7. Gel mobility shift assay

The interaction of complexes with DNA-Topo II was followed by enzyme-mediated supercoiled pBR322 relaxation [54,55]. For activity measurement the reactions were performed in a mixture containing 50 mM Tris–HCl, pH 7.5, 50 mM KCl, 1 mM MgCl₂ 1 mM

ATP, 0.1 mM EDTA, 0.5 mM DTT, 30 μ g/ml BSA and enzyme protein. Supercoiled pBR322 DNA (0.25 μ M) was used as substrate. The reaction mixture was incubated for 30 min at 37 °C and quenched by adding 5 μ L of the loading dye (buffer containing 0.25% bromophenol blue, 1 M sucrose, 1 mM EDTA, and 0.5% SDS). Samples were applied on horizontal 1% agarose gel in 40 mM Tris–acetate buffer, pH 8.3, and 1 mM EDTA and run for 10 h at room temperature at 20 V. The gel was stained with ethidium bromide (0.10 μ g/mL) and photographed in a GDS 7500 UVP (Ultra Violet Product, Cambridge, UK) transilluminator. One unit of topoisomerase activity is defined as the amount of enzyme required to relax 50% of the supercoiled DNA under standard assay conditions.

The B–Z conformational transitions of CT-DNA in presence of **1**, **2**, **3** and **5** were followed spectrophotometrically [56,57]. The absorbance ratio A_{295}/A_{260} was monitored for conformational changes in the DNA helix. Condensation of the DNA was monitored by following the increase in absorbance at 320 nm against different complex/DNA ratios [58–61].

2.8. Heme polymerase assay

Antimalarial activity of **1–5** was investigated by examining their inhibition percentage against β -hematin formation [62]. The reaction mixture (1 mL) contained 100 μ L of 1 M sodium phosphate buffer, 20 μ L of hemin (1.2 mg/mL), and 25 μ L of *P. yoelii* enzyme in triple distilled water. It was treated with 20 μ g complexes followed by incubation for 16 h at 37 °C in an incubator shaker at a speed of 174 rpm. After incubation the reaction mixture was centrifuged at 10,000 rpm for 15 min and the pellets obtained were washed thrice with 10 mL of buffer (containing 0.1 M Tris–HCl, pH 7.5, and 2.5% SDS) and then with buffer 2 (containing 0.1 M sodium bicarbonate, pH 9.2, and 2.5% SDS), followed by distilled water. Semi dried pellets were suspended in 50 μ L of 0.2 N NaOH and volume adjusted to 1 mL with distilled water. The optical density was measured at 400 nm and percent inhibition was calculated using the formula: % inhibition = {(1 – O.D of the control)/O.D experimental} \times 100.

3. Results and discussion

Reactions of the complexes [Ru(κ^3 -L)(PPh₃)Cl₂] (L = tpy and tptz) with hetero difunctional phosphine PPh₂Py (1:2 molar ratio) in methanol under refluxing conditions gave *P*-coordinated cationic complexes [Ru(κ^3 -tpy)(κ^1 -P-PPh₂Py)₂Cl]⁺ (**1**) and [Ru(κ^3 -tptz)(κ^1 -P-PPh₂Py)₂Cl]⁺ (**2**), which were isolated as their tetrafluoroborate salts. Upon treatment with an excess of NH₄PF₆ in methanol at room temperature the complexes **1** and **2** afforded [Ru(κ^3 -tpy)(κ^1 -P-PPh₂Py)(κ^2 -P,N-PPh₂Py)]²⁺ (**4**) and [Ru(κ^3 -tptz)(κ^1 -P-PPh₂Py)(κ^2 -P,N-PPh₂Py)]²⁺ (**5**), wherein one of the coordinated PPh₂Py forms a *P,N*-chelated four membered ring (Schemes 3 and 4).

On the other hand, reaction of [Ru(κ^3 -tpy)Cl₃] with PPh₂Py in 1:1 molar ratio gave the neutral complex [Ru(κ^3 -tpy)(κ^1 -P-PPh₂Py)Cl₂] (**3**) in reasonably good yield (Scheme 5).

The hemi labile nature of coordinated PPh₂Py in these complexes has been established by reacting representative complexes **4** and **5** with an excess of NaCN and CH₃CN in methanol under refluxing conditions. As expected, it gave cationic complexes [Ru(κ^3 -tpy)(κ^1 -P-PPh₂Py)₂(CN)]PF₆ (**6**), [Ru(κ^3 -tpy)(κ^1 -P-PPh₂Py)₂(NCCH₃)](PF₆)₂ (**7**), [Ru(κ^3 -tptz)(κ^1 -P-PPh₂Py)₂(CN)]PF₆ (**8**) and [Ru(κ^3 -tptz)(κ^1 -P-PPh₂Py)₂(NCCH₃)](PF₆)₂ (**9**) in good yield, which were isolated as their hexafluorophosphate salt (Schemes 3 and 4).

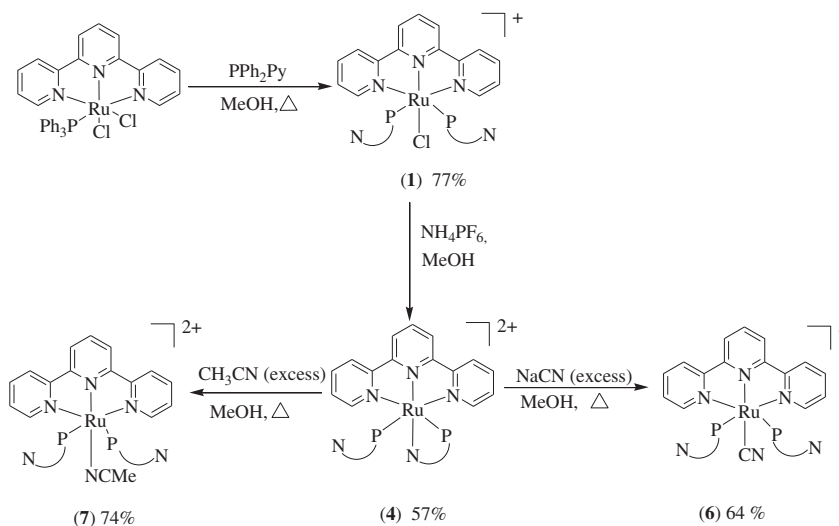
The complexes under study are air stable, non hygroscopic, crystalline solids, soluble in polar solvents such as chloroform, dichloromethane and insoluble in benzene, hexane and *n*-pentane, diethyl ether and petroleum ether. All the complexes have been

Table 1
Rearrangement of various oximes into amides.^a

Entry	R	Time (h)	Yield ^b %
1	(4-NO ₂)C ₆ H ₄	10	82
2	(4-OCH ₃)C ₆ H ₄	10	80
4	(4-CN)C ₆ H ₄	12	80

^a 2.00 mmol of oxime, [Ru(κ^3 -tpy)(PPh₂Py)Cl₂] (1 mol%), and toluene (1 ml) were refluxed for the specified amount of time.

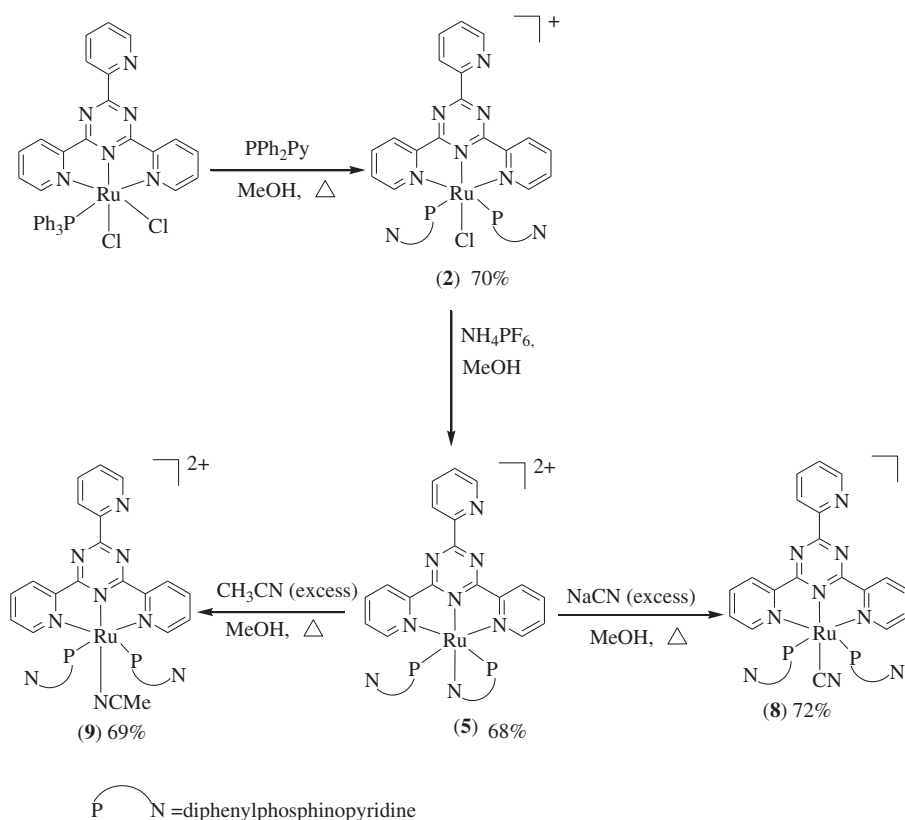
^b Isolated yields after column chromatography.

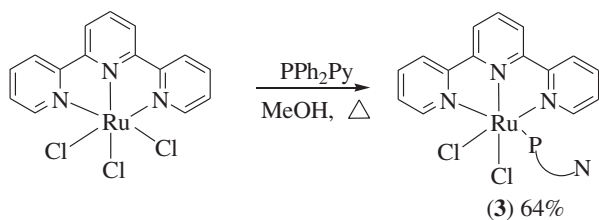
Scheme 3. Synthesis **1**, **4**, **6** and **7**.

characterized by satisfactory elemental analyses, spectral and electrochemical studies. Analytical data of **1–9** conformed well to their respective formulations. Information about the composition of complexes has also been obtained by FAB-MS spectral studies. The MS spectra of **1–5** are depicted in Figure S1–S5 (Supporting Information) and resulting data along with their assignments are summarized in the experimental section. The position of various peaks and overall fragmentation pattern strongly supported proposed formulation of the respective complexes.

3.1. NMR spectral studies

^1H and ^{31}P NMR spectral data summarized in experimental section strongly supported formation of the complexes. Shift in the position of signals associated with tptz and tpy protons relative to these in precursor complexes suggested coordination of PPh_2Py to ruthenium in monodentate/chelating mode. $^{31}\text{P}\{^1\text{H}\}$ NMR spectra provided valuable information about coordination mode of the PPh_2Py in respective complexes. In its $^{31}\text{P}\{^1\text{H}\}$ NMR spectra **1** and **2**

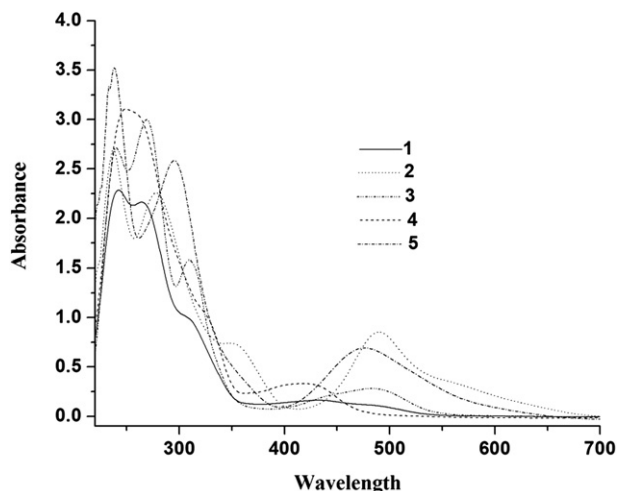
Scheme 4. Synthesis **2**, **5**, **8** and **9**.

Scheme 5. Synthesis of **3**.

displayed singlets at δ 36.02 and 40.04 ppm, assignable to ^{31}P nuclei of the coordinated PPh_2Py . The presence of only one signal indicated that both the ^{31}P nuclei are chemically equivalent and are *trans*-disposed. On the other hand, **4** and **5** displayed singlets in the high field side at δ –10.30 and –12.30 ppm, along with the signals in low field side at δ 36.42 and 38.48 ppm. The presence of resonances both in the high and low field side suggested coordination of PPh_2Py to ruthenium in two different modes. Accordingly the signals in high field side have been assigned to ^{31}P nuclei of chelated κ^2 -*P,N*- PPh_2Py , while the one in down field side to κ^1 -*P*-bonded PPh_2Py . It is interesting to note that in these complexes the ^{31}P nuclei of PPh_2Py exhibited an upfield shift in comparison to the free ligand (δ –3.9 ppm). The upfield shift may be attributed to high electron density on the metal center resulting from coordination of two bulky PPh_2Py ligands. Owing to high electron density on the metal center one can expect enhanced metal-to-ligand $d\pi$ – $p\pi$ back bonding interactions.

3.2. UV–vis spectroscopy

Electronic spectral data of the complexes is summarized in the experimental section and spectra of **1–5** depicted in Fig. 1. Ruthenium polypyridyl complexes usually exhibit intense peaks in ultra violet region attributable to ligand based $\pi \rightarrow \pi^*$ transitions with overlapping MLCT transitions in the visible region [17,63]. Electronic absorption spectra of **1–5** displayed bands at ~554–536, 495–484, ~345–341 and ~286–243 nm. On the basis of its position and intensity the lowest energy transitions in visible region at ~554–539 nm have been assigned to $d\pi(\text{Ru}) \rightarrow \pi^*$ (tptz/tpy) MLCT transitions and the bands at ~495–484 to $d\pi(\text{Ru}) \rightarrow \pi^*$ (PPh_2Py). High energy transitions at ~345–341 and ~286–243 nm have been assigned to intra-ligand charge transfer

Fig. 1. UV–vis spectra of **1–5** in dichloromethane.

$\pi \rightarrow \pi^*/n \rightarrow \pi^*$ transitions [64,65]. Notably, the coordination of PPh_2Py in chelating mode leads to a blue shift in the position of MLCT transition. It may be attributed to enhanced π -back bonding resulting from coordination of one PPh_2Py in chelating mode through both the P and N-donor sites. Further, complexes containing tpy displayed a red shift in the position of lowest energy transitions (~554 nm, **1**; 548 nm, **3**; 539 nm, **4**) in comparison to tptz complexes (536 nm, **2**; 538 nm, **5**). It may be attributed to greater stabilization of the π^* orbitals on tpy relative to tptz. However, introduction of anionic (CN^-) or neutral (NCCH_3) ligands in complex **4** and **5** has little influence on the MLCT bands.

3.3. Electrochemistry

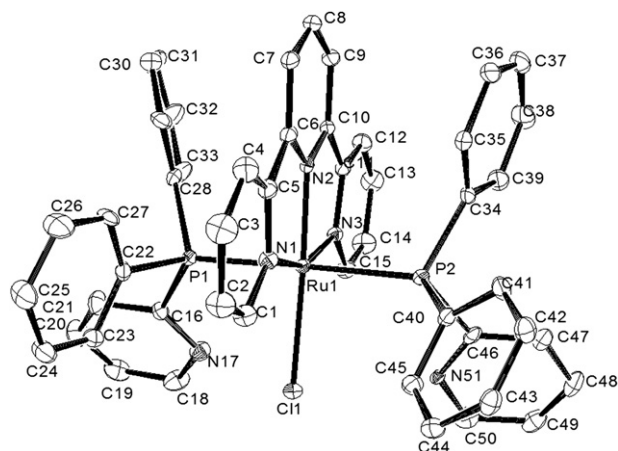
Electrochemical properties of **1–5** in acetonitrile have been followed by cyclic voltammetry using 0.1 M tetrabutylammonium perchlorate (TBAP) as supporting electrolyte. Resulting data is summarized in Table 2 and cyclic voltammograms of **1, 4** and **5** are shown in Figure S6–S8. The potential of Fc/Fc^+ couple under experimental conditions was 0.10 V (80 mV) vs Ag/Ag^+ . The complexes displayed an oxidative wave in the range 0.39–1.15 V [0.62 (90), **1**; 1.15 (92), **2**; 1.10 (74) V, **3**; 0.51 (69), **4**; 0.39 (75), **5**] assignable to $\text{Ru}(\text{II})/\text{Ru}(\text{III})$ oxidation. The peak-to-peak separation (ΔE_p) of ~69 mV and equivalence of the anodic peak current to cathodic peak current (i_{pc}) in **4** and other complexes suggested a reversible electron transfer process. The magnitude of oxidation potential indicated that the bivalent state of ruthenium is comfortable in the *P,N* coordination mode. Further, it has been observed that $\text{Ru}(\text{II})/\text{Ru}(\text{III})$ oxidation potential in complexes **4** and **5** are lower in comparison to those of **1** and **2**. It suggested that PPh_2Py is a better stabilizer of the trivalent state of ruthenium in κ^2 -chelating mode in comparison to monodentate κ^1 -mode in **1** and **2**. It may be due to high electron density on the metal center arising from back bonding between metal and ligand through $p\pi$ – $d\pi$ interactions. The complexes displayed successive three electron reductions at ~ (–) 0.60–1.69 (tptz, complexes), ~ (–) 0.29–1.19 V (tpy, complexes). As the ligand becomes more electron deficient there is concomitant lowering of the ligand LUMO, resulting in an enhanced π -acceptance and more anodic $\text{Ru}^{\text{III/II}}$ oxidation couples.

3.4. X-ray crystallography

Molecular structures of **1, 2** and **3** have been determined crystallographically. ORTEP views at 30% thermal ellipsoid probability along with the atom numbering scheme is shown in Fig. 2–4. Details about data collection, solution and refinement are summarized in Table 3 and important geometrical parameters in Table 4. A common structural feature of **1, 2** and **3** is κ^1 -*P*- PPh_2Py coordination of PPh_2Py to the metal center ruthenium. The coordination geometry about ruthenium in these complexes is distorted octahedral. The bond angles N1–Ru–N2 and N2–Ru–N3 are almost equal [79.68(2) and 79.47(2)°, **1**; 78.72(2) and 78.37(2)°, **2**; 79.14(2), 79.65(2)°, **3**]. It suggested an octahedral distortion due to inward bending of the coordinated pyridyl rings in tptz as well as

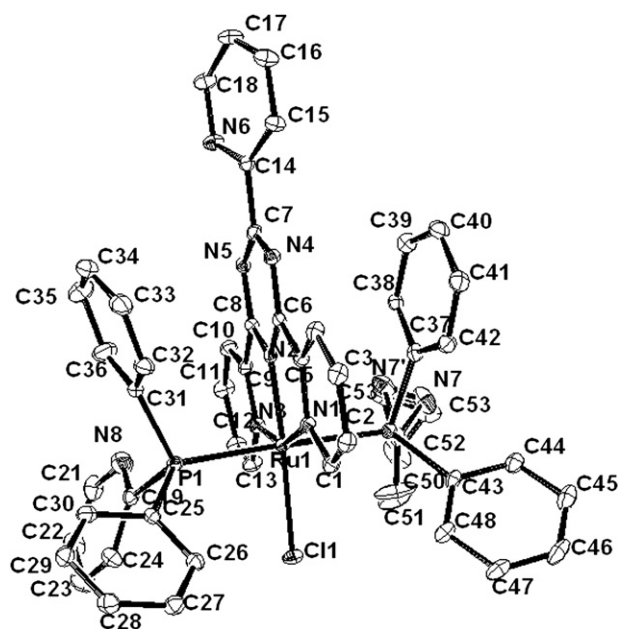
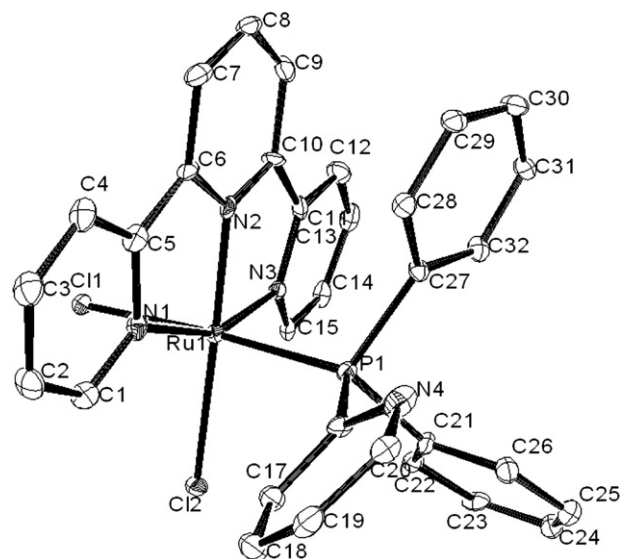
Table 2
Electrochemical data of **1–5** in acetonitrile solution at (rt), scan rate 100 mV/s.

Complex	$E_{1/2}$ (V)	E_p (V)
	Ru II/III	Ligand centered
1	0.62(90)	–0.69, –1.08, –1.36
2	1.10(92)	–0.72, –1.06, –1.69
3	1.15(74)	–0.29, –1.70, –1.99
4	0.51(69)	–0.69, –1.03, –1.28
5	0.39(75)	–0.71, –1.11, –1.49

Fig. 2. Crystal structure of **1**.

tpy complexes. The distortion from regular octahedral geometry is further evidenced from intra-ligand *trans* angles N1–Ru–N3, which are 158.9(15), 157.13(16) and 157.84(17)°, respectively in **1**, **2** and **3**. Other intra-ligand *trans* angles also, supported distorted octahedral geometry about the metal center ruthenium. In complex **3**, the Cl2–Ru–Cl1 angle [87.50(4)°] suggested that coordinated chloro-groups are *cis* disposed. The Ru–Cl and Ru–P bond distances are normal and close to the one reported in other related complexes [49,66]. In compound **1**, the BF₄[−] anion is disordered over two positions with equal S.O.Fs.

The Ru–N bond lengths in **1**, **2** and **3** are normal and consistent with κ^3 -coordination of tptz/tpy to ruthenium [49,66–71]. The uncoordinated pyridyl rings in **1** and **2** are inclined from the central triazine ring plane by 18.14 and 18.6°, respectively. The Ru–Cl1 bond distances in **1** and **2** are indistinguishable (~2.41 Å) and close to reported values whereas in **3** the Ru–Cl1 and Ru–Cl2 distances are slightly longer [(2.44(1) and 2.45(1) Å)] but in the range of Ru–Cl bond distances [67]. The Ru–P bond distances in **1**, **2** and **3** are comparable to the values reported in literature [68].

Fig. 3. Crystal structure of **2**.Fig. 4. Crystal structure of **3**.

Structural studies on **1**, **2** and **3** revealed the presence of extensive intra- and intermolecular C–H···X (X = N, Cl, and F) and C–H··· π interactions. Various interaction distances fall in the normal range [69–71]. Matrices for the weak bonding interactions in **1**, **2** and **3** are given in Table S1 (Supporting Information) and some interesting motifs are shown in Figures S9–S13.

3.5. Absorption titration studies

Absorption titration studies performed on **1** and **3** with calf thymus (CT-DNA) indicated significant interaction between the complexes and nucleic acid. Absorption titration spectra of **1** and **3** are shown in Figure S14–16. Titration of **1** and **3** (1–40 μ M) with a constant concentration of CT-DNA (20 μ M) shows a pronounced increase in the absorption intensities (hyperchromism) at higher concentrations (Figure S15–16). The hyperchromicity implies interactions other than intercalation between the complexes and DNA, because intercalation leads to a hypochromism. It suggested that at higher concentration unwinding of DNA helix leads to an increase in absorption intensity. Further, at lower concentration (5 μ M and 1 μ M) it exhibited a decrease in the absorption intensity (hypochromism) with respect to CT-DNA. At lower concentrations **1** and **3** displayed a pronounced hypochromism at their respective metal-to-ligand charge transfer (MLCT) bands. It may arise from the interaction between electronic state of intercalating chromophore of tpy/tptz and that of DNA bases. The spectral changes at lower concentration are consistent with intercalation of the complexes into DNA base-stack.

3.6. B–Z conversion

Anomalous morphology of Z-DNA and its involvement in gene expression and recombination have drawn extensive scientific attention [57,58]. The B–Z-DNA transition in presence of the complexes under study has been followed spectrophotometrically. Change in the ratio A_{295}/A_{260} is commonly taken as an evidence for conformational changes in the DNA structure. The complexes **1–5** promoted an increase in A_{295}/A_{260} ratio from 0.18 (for free DNA) to 0.77 (**1**), 0.66 (**2**), 0.56 (**3**), 0.72 (**4**) and 0.78 (**5**). The observed alternation in UV absorption ratio in presence of complexes suggested conformational changes in DNA structure. The B–Z equilibrium may be influenced by two major factors, the ionic changes

Table 3
Selected crystallographic data for **1**, **2** and **3**.

	1	2	3
Empirical formula	C ₄₉ H ₃₉ BClF ₄ N ₅ P ₂ Ru	C ₅₂ H ₄₀ BClF ₄ N ₆ OP ₂ Ru	C ₃₃ H ₂₇ Cl ₄ N ₄ PRu
Formula weight	983.12	1078.19	753.43
Temperature (K)	150(2)	150(2)	293(2)
Crystal system	Triclinic	Orthorhombic	Monoclinic
space group	<i>P</i> -1	<i>Pbca</i>	<i>C</i> _{2/c}
Wavelength (Å)	0.71073	0.71073	0.71073
Unit cell dimensions	<i>a</i> = 11.2150(4) Å <i>b</i> = 11.6340(3) Å <i>c</i> = 19.5580(6) Å α = 73.770(3)° β = 85.968(3)° γ = 70.778(3)°	<i>a</i> = 15.4385(3) Å <i>b</i> = 20.1888(5) Å <i>c</i> = 31.0093(6) Å	<i>a</i> = 20.931(2) Å <i>b</i> = 10.3381(10) Å <i>c</i> = 30.490(3) Å β = 108.914(3)°
Volume (Å ³)	2312.88(12)	9665.1(4)	6241.4(11)
Z, Calculated density (g cm ⁻³)	2, 1.412	8, 1.482	4, 0.941
μ (mm ⁻¹)	0.522	0.510	0.389
F(000)	1000	4384	1784
Crystal size (mm)	0.34 × 0.30 × 0.28	0.28 × 0.26 × 0.18	0.28 × 0.26 × 0.21
Theta range for data collection	3.12–25.00 deg.	3.11–25.00	2.08–28.30
Limiting indices	–13 ≤ <i>h</i> ≤ 12 –13 ≤ <i>k</i> ≤ 11 –22 ≤ <i>l</i> ≤ 23	–18 ≤ <i>h</i> ≤ 18 –21 ≤ <i>k</i> ≤ 24 –36 ≤ <i>l</i> ≤ 34	–27 ≤ <i>h</i> ≤ 24 –10 ≤ <i>k</i> ≤ 13 –40 ≤ <i>l</i> ≤ 39
Reflections collected/unique	17988/8116 [R(int) = 0.0304]	35207/8484 [R(int) = 0.0478]	19744/7687 [R(int) = 0.0476]
Data/restraints/parameters	8116/12/593	8484/12/659	7687/0/613
Goof	1.082	1.034	1.366
Final <i>R</i> indices [<i>I</i> > 2σ(<i>I</i>)]	<i>R</i> ₁ = 0.0712 <i>wR</i> ₂ = 0.2226	<i>R</i> ₁ = 0.0540, <i>wR</i> ₂ = 0.1453	<i>R</i> ₁ = 0.0599 <i>wR</i> ₂ = 0.1645
<i>R</i> indices (all data)	<i>R</i> ₁ = 0.0927 <i>wR</i> ₂ = 0.2360	<i>R</i> ₁ = 0.0849 <i>wR</i> ₂ = 0.1551	<i>R</i> ₁ = 0.0911 <i>wR</i> ₂ = 0.2197

in solution and covalent modification [72,73]. Further, condensation of the calf thymus (CT-DNA) promoted by **1–5** was monitored spectrophotometrically following the increase in absorption at 320 nm [59–62]. The complexes **1–5** exhibited condensation of DNA at 20 μM concentration level, which is evident from enhancement in the absorption at 320 nm [A_{320}/A_{260}] from 0.075 for free DNA to 0.38 (**1**), 0.28 (**2**), 0.53 (**3**), 0.49 (**4**) and 0.45(**5**). It was observed that **3**, **4** and **5** are more effective in this regard in comparison to **1** and **2**.

3.7. Gel mobility assays

Direct DNA–metal interactions are evidenced by change in electrophoretic mobility of the plasmid DNA on agarose gel [7,8].

Alteration in the structure of DNA leads to retardation in migration of supercoiled DNA and slight increase in mobility of the open circular DNA. It has been shown that topo II is an essential enzyme which plays an important role in DNA replication, repair and transcription [74,75]. It is well known that non-covalent interaction of the proteins with DNA is key step in Topo II catalytic cycle. Anti-Topo II agents control the Topo II activity either by trapping Topo II-DNA complex or acting as Topo II inhibitors [76–79]. The effect of **1–5** on Topo II activity of the filarial parasite *S. cervi* was followed by enzyme-mediated supercoiled pBR322 relaxation assay [51,52]. Gel mobility assays of **1–5** were examined at different concentration levels. These complexes do not show DNA binding in absence of enzyme Topo II (Figure S17–S18). However, in the presence of Topo II an upward shift toward relaxed form of the plasmid DNA to

Table 4
Selected geometrical parameters for **1**, **2** and **3**.

1	2	3
Ru(1)–N(2) 1.967(5)	Ru(1)–N(2) 1.931(4)	Ru(1)–N(2) 1.961(4)
Ru(1)–N(1) 2.085(5)	Ru(1)–N(3) 2.081(4)	Ru(1)–N(3) 2.070(4)
Ru(1)–N(3) 2.103(5)	Ru(1)–N(1) 2.114(4)	Ru(1)–N(1) 2.087(4)
Ru(1)–P(2) 2.3636(17)	Ru(1)–P(1) 2.3812(15)	Ru(1)–P(1) 2.3041(13)
Ru(1)–P(1) 2.3883(17)	Ru(1)–P(2) 2.3864(15)	Ru(1)–Cl(1) 2.4431(13)
Ru(1)–Cl(1) 2.4616(17)	Ru(1)–Cl(1) 2.4345(13)	Ru(1)–Cl(2) 2.4548(12)
N(2)–Ru(1)–N(1) 79.8(15)	N(2)–Ru(1)–N(3) 78.39(16)	N(2)–Ru(1)–N(3) 79.65(17)
N(2)–Ru(1)–N(3) 79.2(15)	N(2)–Ru(1)–N(1) 78.78(16)	N(2)–Ru(1)–N(1) 79.14(17)
N(1)–Ru(1)–N(3) 158.9(15)	N(3)–Ru(1)–N(1) 157.13(16)	N(3)–Ru(1)–N(1) 157.84(17)
N(2)–Ru(1)–P(2) 90.16(15)	N(2)–Ru(1)–P(1) 91.21(12)	N(1)–Ru(1)–P(1) 93.65(11)
N(1)–Ru(1)–P(2) 90.05(16)	N(3)–Ru(1)–P(1) 89.71(13)	N(3)–Ru(1)–Cl(1) 87.37(11)
N(3)–Ru(1)–P(2) 90.65(15)	N(1)–Ru(1)–P(2) 91.99(12)	N(2)–Ru(1)–Cl(1) 91.06(11)
N(2)–Ru(1)–P(1) 91.20(15)	N(2)–Ru(1)–P(2) 91.19(12)	N(1)–Ru(1)–Cl(1) 86.63(11)
N(1)–Ru(1)–P(1) 90.59(16)	N(3)–Ru(1)–P(2) 89.70(13)	N(3)–Ru(1)–Cl(2) 99.67(12)
N(3)–Ru(1)–P(1) 89.22(15)	N(1)–Ru(1)–P(2) 89.27(12)	N(2)–Ru(1)–Cl(2) 178.44(12)
P(2)–Ru(1)–P(1) 178.59(7)	P(1)–Ru(1)–P(2) 177.36(5)	N(1)–Ru(1)–Cl(2) 101.36(12)
N(2)–Ru(1)–Cl(1) 175.92(16)	N(2)–Ru(1)–Cl(1) 174.43(12)	P(1)–Ru(1)–Cl(1) 176.79(4)
N(1)–Ru(1)–Cl(1) 96.29(17)	N(3)–Ru(1)–Cl(1) 96.39(12)	P(1)–Ru(1)–Cl(2) 89.39(4)
N(3)–Ru(1)–Cl(1) 104.75(16)	N(1)–Ru(1)–Cl(1) 106.47(12)	Cl(1)–Ru(1)–Cl(2) 87.50(4)
P(1)–Ru(1)–Cl(1) 87.78(6)	P(1)–Ru(1)–Cl(1) 86.79(5)	N(2)–Ru(1)–P(1) 92.14(11)
P(2)–Ru(1)–Cl(1) 90.90(6)	P(2)–Ru(1)–Cl(1) 90.71(5)	N(3)–Ru(1)–P(1) 93.51(11)

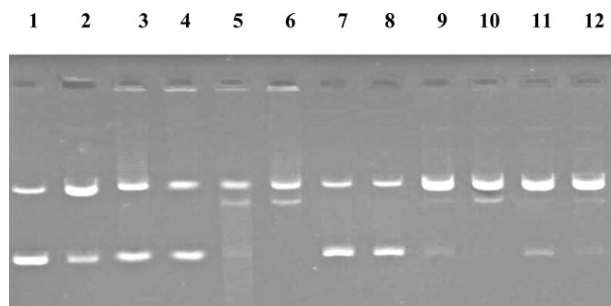


Fig. 5. Gel mobility shift assay of *S. cerevisiae* topoisomerase II by the complexes **1**, **2**, **3**, **4** and **5** (20 μg, lane 3, 6, 7, 9 and 11; 40 μg, lane 4, 5, 8, 10, and 12) Lane 1: Supercoiled pBR322 (0.2 μg) alone; Lane 2: Supercoiled pBR322 + *S. cerevisiae* topo II; Lane 3–4: **1**; Lane 5–6: **4**; lane 7–8: **2**; lane 9–10: **5**; and lane 11–12: **3**.

gel origin indicated that the complexes influence Topo II-DNA activity by binding either to Topo II-DNA complex or the enzyme. An appreciable effect on DNA activity has been observed by substitution of the chloro group of precursor complexes $[\text{Ru}(\kappa^3\text{-tptz})\text{Cl}_2(\text{PPh}_3)]$, $[\text{Ru}(\kappa^3\text{-tpy})(\text{PPh}_3)\text{Cl}_2]$ and $[\text{Ru}(\kappa^3\text{-tpy})\text{Cl}_3]$ by PPh_2Py . Further, it was observed that complex **1** inhibited Topo II activity at 40 μM per reaction mixture in presence of the enzyme. At the same concentration level (40 μM) it exhibited strong complex formation ability with DNA-Topo II complex as indicated by the presence of DNA in gel lane (Figs. 5 and 6). On the other hand, **2** exhibited high Topo II inhibitory activity at 10, 20 and 40 μM levels (Figs. 5 and 7). It suggested that at higher concentration **1** and **2** inhibited relaxation of the supercoiled DNA, displaying a significant inhibitory activity. Further, it was observed that **3**, **4** and **5** are not effective in this regard. This may result from structural changes and ligands (tpy and tptz) involved in complex. It is observed that inhibitory activity is dependent upon the number of coordinated and uncoordinated nitrogen donor atoms. The complex **2** possesses 8 pyridyl nitrogens among which, only three are involved in coordination and other five remains uncoordinated. On the other hand, **1** has only two uncoordinated pyridyl nitrogens. Higher inhibition displayed by complex **2** in comparison to **1** strongly suggested that inhibitory activity is determined by number of uncoordinated nitrogen atoms. Ru(II) complexes used in the present study are octahedral, wherein coordination geometry is completed by the pyridyl nitrogen from ligands (tpy/tptz) along with two PPh_2Py lying *trans* to each other. An inspection of the single crystal X-ray structure of **1** or **2** reveals that planar part of the ligand may stack between base pairs of the DNA major groove. In **4** and **5** one of the

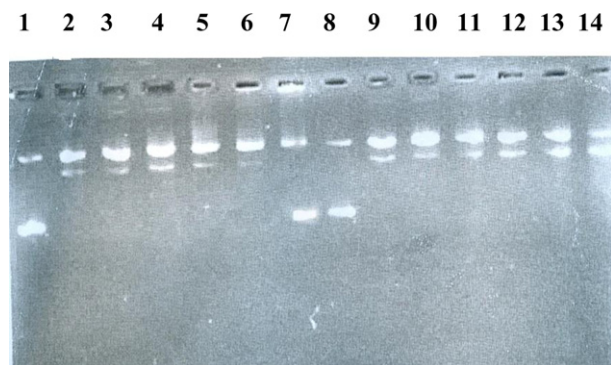


Fig. 6. Gel mobility shift assay of *S. cerevisiae* topoisomerase II by the complexes **1** and **4**: (2 μg, lane 3 and 10, 5 μg, lane 4 and 11, 10 μg, lane 5 and 12, 20 μg, lane 6 and 13, 40 μg, lane 7 and 14) Lane 1 and 8: Supercoiled pBR322 (0.2 μg) alone; Lane 2 and 9: Supercoiled pBR322 + *S. cerevisiae* topo II; Lane 3–7: **1**; Lane 10–14: **4**.

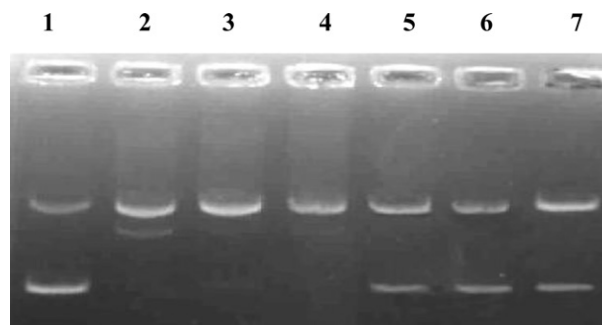


Fig. 7. Gel mobility shift assay of *S. cerevisiae* topoisomerase II by the complex **2** (2 μg, lane 3; 5 μg, lane 4; 10 μg, lane 5; 20 μg, lane 6; 40 μg, lane 7). Lane 1: Supercoiled pBR322 (0.2 μg) alone; Lane 2: Supercoiled pBR322 + *S. cerevisiae* topo II.

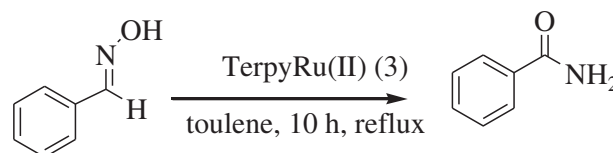
coordinated PPh_2Py interacted with metal center in a chelating mode forming a four membered ring. The lower inhibition activity of **3**, **4** and **5** may be attributed to an increase in steric hindrance resulting from the replacement of chloro group leading to the formation of four membered chelate rings or introduction of bulkier PPh_2Py .

3.8. Heme polymerase activity

The complexes **1–5** also exhibited significant inhibitory effect on heme polymerase activity of *P. yoelii* lysate, which was followed by β-hematin formation [63]. The parent complex $[\text{Ru}(\kappa^3\text{-tptz})\text{Cl}_2(\text{PPh}_3)]$ shows 94% inhibition of heme polymerase activity, while **1–5** exhibited lower inhibition percentage (50, **1**; 50, **2**; 62, **3**; 56, **4** and 54, **5**). The above results could be attributed to an increase in the steric hindrance resulting from replacement of the chloro group in the complexes $[\text{Ru}(\kappa^3\text{-tpy})\text{Cl}_2(\text{PPh}_3)]$ and $[\text{Ru}(\kappa^3\text{-tptz})\text{Cl}_2(\text{PPh}_3)]$ by bulkier PPh_2Py ligand.

3.9. Catalytic applications of $[\text{Ru}(\kappa^3\text{-tpy})(\kappa^1\text{-P-PPh}_2\text{Py})\text{Cl}_2]$ (**3**) in the rearrangement of the aldoximes to amide

It is well known that the oximes are less amenable to reduction in comparison to imines, although Beckmann rearrangement catalytic pathways can be employed to convert alcohols into hydroxylamines. In this study we have developed ruthenium polypyridyl complexes containing PPh_2Py as a co-ligand, which catalyses conversion of oximes to amide. The representative complex **3** has been successfully employed as a catalyst for conversion of oximes to amide (Scheme 6) in absence of an alcohol or base. The optimized reaction conditions may be employed for the conversion of a range of oximes into corresponding amides (Table S4). Benzaldehyde oxime upon treatment with **3** (1 mol %) in toluene under refluxing conditions (for 10 h, Scheme 6) gave benzamide in 80% yield. The yields of isolated amides after simple purification are consistently excellent (Table S4). Notably in this reaction benzonitrile the product of abnormal Beckmann rearrangement sometimes seen in the transition metal-catalyzed reactions was not observed [40,80–84]. Further, additional acid



Scheme 6. Rearrangement of benzaldehyde oxime to benzamide.

or base was not required and addition of K_2CO_3 or *p*-toluene sulfonic acid brought down the yield of amide. The conversion of aldoximes to amides, especially, under such mild conditions is a desirable process, as carbonyl compounds are readily available. This reaction has been reported earlier using Pd, Ni, Mn, and Rh [84] catalysts however these use either toxic reagents or elevated temperature [81–84]. From mechanistic point of view it is interesting to note that O-alkylated oximes are inert to reaction as these are derived from ketones. It suggested that the presence of both hydrogen and a hydroxyl group is essential for the transformations. In addition, nitrones are also resistant to rearrangement. Further, benzonitrile was inert to hydrolysis under these reaction conditions, suggesting that the reaction does not proceed via a free nitrile. Several mechanisms could be conceived for this process, one such mechanism may involve initial displacement of a chloride by oxime allowing the ruthenium to remove oxygen and hydride, followed by replacing them in the isomeric form prior to release of the amide.

4. Conclusions

In this work we have described the synthesis and characterization of some ruthenium(II) complexes containing polypyridyl ligands like 2,2':6',2''-terpyridine (tpty) or 2,4,6-tris(2-pyridyl)-1,3,5-triazine (tptz) and diphenyl-2-pyridylphosphine (PPh₂Py) as co-ligand. It has been shown that depending upon requirements about the metal center PPh₂Py may interact with the ruthenium in κ^1 -P-PPh₂Py or chelating κ^2 -P,N bonding mode. Absorption titration and gel electrophoretic studies have shown that the complexes **1** and **2** exhibit good inhibitory activities against DNA-Topo II of the filarial parasite *S. cervi* at higher concentrations while **3**, **4** and **5** are not effective in this regard. These also exhibit heme polymerase activity against malarial parasite *P. yoelii*. In addition, it has been shown that complex **3** catalyses conversion of oximes into amide under mild conditions.

Acknowledgements

Financial support from the Department of Science and Technology, Ministry of Science and Technology, New Delhi, India (Grant No. SR/SI/IC-15/2007) is gratefully acknowledged. We are also thankful to Prof. P. Mathur, In-charge, National Single Crystal X-ray Diffraction Facility, Indian Institute of Technology, Mumbai for providing single crystal X-ray data.

Appendix. Supporting information available

Supplementary data associated with this article can be found, in the online version, at doi:10.1016/j.jorganchem.2011.06.031.

Abbreviations

tpty = 2,2':6',2''-terpyridine
 tptz = 2,4,6-tris(2-pyridyl)-1,3,5-triazine
 PPh₂Py = diphenyl-2-pyridylphosphine
 DNA-Topo II = deoxyribose nucleic acid – Topo isomerase II
 MLCT = metal-to-ligand charge transfer
 TBAP = Tetrabutylammonium perchlorate
 CT-DNA = calf thymus DNA

References

[1] V. Balzani, A. Juris, M. Venturi, S. Campagna, F. Puntariero, S. Serroni, Coord. Chem. Rev. 219 (2001) 545–572.

[2] K. Chichak, U. Jacquemard, N.R. Branda, Eur. J. Inorg. Chem. (2002) 357–368.
 [3] X.W. Liu, J. Li, H. Deng, K.C. Zheng, Z.W. Mao, L.N. Ji, Inorg. Chim. Acta. 358 (2005) 3311–3319.
 [4] C.A. Puckett, J.K. Barton, J. Am. Chem. Soc. 129 (2007) 46–47.
 [5] A. Sigel, H. Sigel (Eds.), Metal Ions in Biological Systems, vol. 33, Marcel Dekker, New York, 1996.
 [6] K.E. Erkkila, D.T. Odum, J.K. Barton, Chem. Rev. 99 (1999) 2777–2795.
 [7] C.J. Elsevier, J. Reedijk, P.H. Walton, M.D. Ward, Dalton Trans. (2003) 1869–1880.
 [8] K.D. Demadis, C.M. Hartshorn, T.J. Meyer, Chem. Rev. 101 (2001) 2655–2686.
 [9] M.I.J. Polson, E.A. Medlycott, G.S. Hanan, L. Mikelsons, N.J. Taylor, M. Watanabe, Y. Tanaka, F. Loiseau, R. Passalacqua, S. Campagna, Chem. Eur. J. 10 (2004) 3640–3648.
 [10] C.M. Metcalfe, S. Spey, H. Adams, J.A. Thomas, J. Chem. Soc., Dalton Trans. (2002) 4732.
 [11] A. Amboise, B.J. Maiya, Inorg. Chem. 39 (2000) 4256–4263.
 [12] X.-J. Yang, F. Drepper, B. Wu, W. Sun, W. Haehnel, C. Janiak, Dalton Trans. (2005) 256.
 [13] K. Karidi, A. Garoufis, N. Hadjilidis, J. Reedijk, Dalton Trans. (2005) 728–734.
 [14] M. Sironi, Mol. Biochem. Parasitol. 74 (1995) 223–227.
 [15] S.K. Singh, S. Sharma, M. Chandra, D.S. Pandey, J. Organomet. Chem. 690 (2005) 3105–3110.
 [16] P. Paul, B. Tyagi, A.K. Bilakhiya, P. Dastidar, E. Suresh, Inorg. Chem. 39 (2000) 14–22.
 [17] S. Sharma, S.K. Singh, D.S. Pandey, Inorg. Chem. 47 (2008) 1179–1181.
 [18] A. Maisonnat, J.P. Farr, A.L. Balch, Inorg. Chim. Acta 53 (1981) L217–L218.
 [19] N.M. Alcock, P. Moore, P.A. Lampe, K.F. Mok, Dalton Trans. (1982) 207–210.
 [20] L. Hirsivaara, M. Haukka, J. Pursiainen, Inorg. Chem. Commun. 3 (2000) 508–510.
 [21] C.G. Arena, E. Rotondo, F. Faraone, Organometallics 10 (1991) 3877–3885.
 [22] P. Braunstein, D.G. Kelly, A. Tiripicchio, F. Ugozzoli, Bull. Soc. Chim. Fr. 132 (1995) 1083–1086.
 [23] P. Kumar, A.K. Singh, D.S. Pandey, J. Organomet. Chem. 694 (2009) 3643–3652.
 [24] N.D. Jones, K.S. MacFarlane, M.B. Smith, R.P. Schutte, S.J. Rettig, B.R. James, Inorg. Chem. 38 (1999) 3956–3966.
 [25] M.M. Olmstead, A. Maisonnat, J.P. Farr, A.L. Balch, Inorg. Chem. 20 (1981) 4060–4064.
 [26] S.-L. Li, T.C.W. Mak, Z.-Z. Zhang, Dalton Trans. (1996) 3475.
 [27] E. Freiberg, W.M. Davis, T. Nicholson, A. Davison, A.G. Jones, Inorg. Chem. 41 (2002) 5667.
 [28] M.L. Clarke, A.M.Z. Slawin, M.V. Wheatley, J.D. Woollins, J. Chem. Soc., Dalton Trans. (2001) 3421.
 [29] J.P. Farr, M.M. Olmstead, F. Wood, A.L. Balch, J. Am. Chem. Soc. 105 (1983) 792–798.
 [30] J. Baur, H. Jacobsen, P. Burger, G. Artus, H. Berke, L. Dahlenburg, Eur. J. Inorg. Chem. (2000) 1411–1422.
 [31] T. Suzuku, T. Kuchiyama, S. Kishi, S. Kaizaki, M. Kato, Bull. Chem. Soc. Jpn. 75 (2002) 2433–2439.
 [32] E. Drent, P. Arnoldy, P.H.M. Budzelaar, J. Organomet. Chem. 455 (1993) 247–253.
 [33] C.S. Consorti, G. Ebeling, J. Dupont, Tetrahedron Lett. 43 (2002) 753–755.
 [34] N.A. Owston, A.J. Parker, J.M.J. Williams, Org. Lett. 9 (2007) 73–75.
 [35] S. Park, Y. Choi, H. Han, S.H. Yang, S.B. Chang, Chem. Commun. 15 (2003) 1936–1937.
 [36] M.J. Palmer, M. Wills, Tetrahedron: Asymm. 10 (1999) 2045–2061.
 [37] S. Sakaguchi, T. Yamaga, Y. Ishii, J. Org. Chem. 66 (2001) 4710–4712.
 [38] N. Uematsu, A. Fujii, S. Hashiguchi, T. Ikariya, R. Noyori, J. Am. Chem. Soc. 118 (1996) 4916–4917.
 [39] N.A. Owston, A.J. Parker, J.M.J. Williams, Org. Lett. 9 (2007) 3599–3601.
 [40] M.B. Smith, J. March, March's Advanced Organic Chemistry. Wiley-Interscience, New York, 2007, vol. 6.
 [41] A. Czap, F.W. Heinemann, R. van Eldik, Inorg. Chem. 43 (2004) 7832–7843.
 [42] C.M. Che, C. Ho, T.C. Lau, J. Chem. Soc., Dalton Trans. (1991) 1901–1907.
 [43] E. Baranoff, J.P. Collin, L. Flamigni, J.P. Sauvage, Chem. Soc. Rev. 33 (2004) 147–155.
 [44] P. Pechy, F.P. Rotzinger, M.K. Nazeeruddin, O. Kohle, S.M. Zakeeruddin, R. Humphrybaker, M. Gratzel, J. Chem. Soc., Chem. Commun. (1995) 65–66.
 [45] U.S. Schubert, H. Hofmeier, G.R. Newkome, Modern Terpyridine Chemistry. Wiley-VCH, Weinheim, 2006.
 [46] G. Chelucci, A. Saba, D. Vignola, C. Solinas, Tetrahedron 57 (2001) 1099–1104.
 [47] F. Fagalde, N.D. Lis De Katz, N.E. Katz, J. Coord. Chem. 55 (2002) 587–593.
 [48] X. Sala, N. Santana, I. Serrano, E. Plantalech, I. Romero, M. Rodriguez, A. Lobet, S. Jansat, M. Gomez, X. Fontrodona, Eur. J. Inorg. Chem. (2007) 5207–5214.
 [49] D.D. Perrin, W.L.F. Armango, D.R. Perrin, Purification of Laboratory Chemicals. Pergamon, Oxford, U.K, 1986.
 [50] B.P. Sullivan, J.M. Calvert, T.J. Meyer, Inorg. Chem. 19 (1980) 1404–1407.
 [51] U. Pandya, J.K. Saxena, S.M. Kaul, P.K. Murthy, R.K. Chatterjee, R.P. Tripathi, A.P. Bhaduri, O.P. Shukla, Med. Sci. Res. 27 (1999) 103–106.
 [52] D.A. Burden, N. Osheroff, Biochim. Biophys. Acta 1400 (1998) 139.

- [53] G.M. Sheldrick, SHELX-97: Programme for The Solution and Refinement of Crystal Structures. University of Göttingen, Germany, 1997.
- [54] A.L. Spek, *Acta Crystallogr.* 46 (1990) C31.
- [55] J.H.K.K. Hirschberg, L. Brunsveld, A. Ramzi, J.A.J.M. Vekemans, R.P. Sijbesma, E.W. Meijer, *Nature* 407 (2000) 167–170.
- [56] D.A. Burden, Osheroff, *Biochim, Biophys. Acta* 1400 (1998) 139–154.
- [57] E.M. Pohl, T.M. Jovin, *J. Mol. Biol.* 67 (1972) 375–396.
- [58] J.B. Chaires, *J. Biol. Chem.* 261 (1986) 8899 and references therein.
- [59] H.S. Basu, L.J. Marton, *Biochem. J.* 244 (1987) 243–246.
- [60] T.J. Thomas, R.P.J. Messner, *Mol. Biol.* 201 (1988) 463.
- [61] M.J. Clarke, F. Zhu, D.R. Frasca, *Chem. Rev.* 99 (1999) 2511.
- [62] H. Chen, J.A. Parkinson, R.E. Morris, P.J. Sadler, *J. Am. Chem. Soc.* 125 (2003) 173.
- [63] A.V. Pandey, N. Singh, B.L. Takwani, S.K. Puri, V.S. Chauhan, *J. Pharma Biomed. Anal.* 20 (1999) 203–207.
- [64] W.J. Perez, C.H. Lake, R.F. See, L.M. Toomey, M.R. Churchill, K.J. Takeuchi, C.P. Radano, W.J. Boyko, C.A. Bessel, *J. Chem. Soc., Dalton Trans.* (1999) 2281.
- [65] P. Didier, I. Ortmans, A.K. Mesmaeker, R.J. Watts, *Inorg. Chem.* 32 (1993) 5239–5245.
- [66] B.P. Sullivan, D.J. Salmon, T.J. Meyer, *Inorg. Chem.* 17 (1978) 3334–3341.
- [67] T.J. Meyer, H. Taube, *Inorg. Chem.* 7 (1968) 2369.
- [68] M. Chandra, A.N. Sahay, D.S. Pandey, R.P. Tripathi, J.K. Saxena, V.J.M. Reddy, M.C. Puerta, P. Valerga, *J. Organomet. Chem.* 689 (2004) 2256–2267.
- [69] H. Aneetha, P.S. Zacharias, B. Srinivas, G.H. Lee, Y. Wang, *Polyhedron* 18 (1999) 299–307.
- [70] G.R. Desiraju, T. Steiner, *The Weak Hydrogen Bond in Structural Chemistry and Biology*. Oxford University Press, Oxford, 1999, 528 pages.
- [71] T. Steiner, *Angew. Chem. Int. Ed.* 41 (2000) 48.
- [72] H. Yin, G.I. Lee, H.S. Park, G.A. Payne, J.M. Rodriguez, S.M. Sebt, A.D. Hamilton, *Angew. Chem., Int. Ed.* 44 (2005) 2704.
- [73] R.E. Morris, R.E. Aird, P.del S. Murdoch, H. Chen, J. Cummings, N.D. Hughes, S. Parsons, A. Parkin, G. Boyd, D.I. Jodrell, P.J. Sadler, *J. Med. Chem.* 44 (2001) 3616–3621.
- [74] A. Johnson, Y. Qu, B.V. Houten, N. Farrell, *Nucleic Acid Res.* 20 (1992) 1697–1703.
- [75] C. Moucheron, *New J. Chem.* 33 (2009) 235–245.
- [76] J.C. Wang, *J. Biol. Chem.* 266 (1991) 6659–6662.
- [77] Y.N. Gopal, D. Jayaraju, A.K. Kondapi, *Biochemistry* 38 (1999) 4382–4388.
- [78] F. Gao, H. Chao, L.-N. Ji, *Chemistry & Biodiversity* 5 (2008) 1962–1979.
- [79] K.-Jie Du, J.-Quan Wang, J.-Feng Kou, G.-Ying Li, L.-Li Wang, H. Chao, L.-Nian Ji, *Eur. J. Med. Chem.* 46 (2011) 1056–1065.
- [80] K. Ishihara, Y. Furuya, H. Yamamoto, *Angew. Chem., Int. Ed.* 41 (2002) 2983–2986.
- [81] S.H. Yang, S.B. Chang, *Org. Lett.* 3 (2001) 4209–4211.
- [82] K. Nakagawa, T. Nakata, R. Konaka, *J. Org. Chem.* 27 (1962) 1597–1601.
- [83] H. Fujiwara, Y. Ogasawara, K. Yamaguchi, N. Mizuno, *Angew. Chem., Int. Ed.* 46 (2007) 5202–5205.
- [84] G.K. Jnaneshwara, A. Sudalai, V.H. Deshpande, *J. Chem. Res., Synop.* (1998) 160–161.